www.gi.sanu.ac.rs, www.doiserbia.nb.rs
J. Geogr. Inst. Cvijic. 2022, 72(2), pp. 133–145

Original scientific paper

UDC: 911.2:007(497.2)
https://doi.org/10.2298/IJGI2202133N

Received: April 16, 2022
Reviewed: June 3, 2022
Accepted: June 13, 2022

GEOINFORMATION TECHNOLOGIES IN THE EVALUATION OF SHORT-TERM GEOMORPHIC CHANGE: AN EXAMPLE OF DAMDERE DEBRIS FLOOD AREA (BULGARIA)

Valentina Nikolova[1]*, *Asparuh Kamburov*[2]

[1]University of Mining and Geology "St. Ivan Rilski", Faculty of Geology and Exploration, Department of Geology and Geoinformatics, Sofia, Bulgaria; e-mail: v.nikolova@mgu.bg
[2]University of Mining and Geology "St. Ivan Rilski", Faculty of Mining Technology, Department of Mine Surveying and Geodesy, Sofia, Bulgaria; e-mail: asparuh.kamburov@mgu.bg

Abstract: A debris flood is a hazardous hydrogeomorphic process that can change the topographic surface in a short time due to a high streamflow and a large volume of sediment transport. Large areas of the Eastern Rhodopes Mountains (Bulgaria) are susceptible to erosion, debris flows, and debris floods due to loose earth masses, rare vegetation, and alternating dry and wet periods with extreme rainfall. The study area is located in the lower part of the river Damdere catchment and covers the area around the check dam. Studying the geomorphic changes of the debris flood areas can provide information about the behavior of the event, and contribute to the development of mitigation measures. In the current research, the data are obtained using terrestrial laser scanning (TLS) during two campaigns (in October 2019 and August 2021). After processing the raw TLS data, two pairs of ground point clouds have been obtained—for the area immediately before the check dam and for the one after the dam. To evaluate the changes in the topographic surface, two approaches are applied: (1) measuring the distance between the successive point clouds (M3C2 algorithm) and (2) measuring the differences between the digital terrain models in geographic information system environment (DoD method). Both approaches have shown similar results and indicated active hydrogeomorphic processes. The relatively large volume of deposition after the check dam is an indicator for the decrease in the retaining capacity of the check dam, which is a prerequisite for the increase of a flood risk.

Keywords: debris flood; TLS; point cloud; GIS; topographic change

1. Introduction

A debris flood is a hydrogeomorphic process in mountain catchments characterized as a flood with a high volume of sediment load, in the ranges 20 to 50–60% (Costa, 1984, 1988; Pierson & Costa, 1987) and 20 to 47% (Wilford et al., 2004) of the flow volume. The event is often related to a debris flow (a rapid movement of highly water-saturated earth masses, proluvial and colluvial materials) and can be considered an intermediate process between a debris flow and a flood. Although the possible adverse impact of a debris flood on infrastructure and ecosystems, and even on human life, debris floods are relatively rarely studied and are rather

*Corresponding author, e-mail: v.nikolova@mgu.bg

considered debris flows. Understanding the nature of debris floods is important for planning and implementing the prevention and mitigation measures.

The analysis of the published materials on this topic shows that some publications consider the basins morphometry to differentiate hydrogeomorphic processes (Bovis & Jakob, 1999; Ilinca, 2021; Jackson et al., 1987; Wilford et al., 2004). The most often used indicators for this purpose are basin relief, Melton index, watershed length, and slope. Attention is also given to the grain size and sorting of debris deposits, as well as the clasts orientation (Ilinca, 2021; Pierson, 2005; Wilford et al., 2004; Zhou et al., 2015). Another indicator are the hydro-geomorphological properties of the area. Slaymaker (1988) considers a debris torrent in relation to channelized debris flows and debris floods. Characterizing the torrential floods in Serbia, Petrović et al. (2014, 2021) direct the attention to its sudden appearance and specific hydrologic and sediment regime.

Most of the publications about hydrogeomorphic processes in Bulgaria and particularly about debris flows consider the conditions and triggering factors for these hazardous events as well as the sedimentological properties of the deposits (Baltakova et al., 2018; Dobrev & Georgieva, 2010; Kenderova et al., 2013; Krenchev et al., 2021; Rizova & Nikolova, 2021). Only a few publications in Bulgaria emphasize on the types of the events (debris flow, debris flood, mud flow, etc.) and on the geomorphic change of the affected areas (Dotseva et al., 2021; Kenderova et al., 2013; Nikolova et al., 2020). In many cases, the term "torrential floods" is used to refer to debris flows and debris floods.

Better understanding of the debris floods and debris flows, and evaluation of the caused topographic change, can be achieved through consistent monitoring of the affected area. In this relation, the application of geospatial technologies provides great opportunities (Aigner et al., 2021; Blasone et al., 2014; Dhote et al., 2022; Kamburov & Nikolova, 2020; Keilig et al., 2018; Loye et al., 2016; Nikolova, Matev, & Pophristov, 2021). The application of terrestrial laser scanning (TLS) allows rapid collection of high-accuracy data used for building high-resolution terrain models and the evaluation of geomorphic change by consecutive scanning in different periods (Li et al., 2021; Picco et al., 2013; Rainato et al., 2013; Schürch et al., 2011). This approach is used in the current study with the aim to analyze the short-term topographic change, driven by debris flood in a small mountain catchment. The area of interest is a part of the river Damdere catchment, located in southern Bulgaria (the Eastern Rhodopes Mountains). Due to the natural conditions of the region (intensive rainfall, rapid snowmelt, and loose sediments), the area is highly susceptible to hydrogeomorphological hazards like debris flows, debris floods, floods, and landslides (Bruchev et al., 2001; Dobrev at al., 2013; Nikolova, Matev, & Pophristov, 2021). Despite the high susceptibility to hazardous events, there is no regular monitoring in this area, which increases a natural disaster risk. In this case, there are no hydrometeorological measurements or the measurement of sediment transport in the catchment of the river Damdere. The evaluation of the topographic change of the debris flood area would give information about the distribution of erosion and accumulation and about the intensity of the hydrogeomorphic processes. New data about the spatio-temporal dynamic of debris floods in the downstream of the river are obtained as a result of the study, which is of importance for better management of the natural hazards.

The applied geoinformation approach and the obtained results are in compliance with other studies on this topic (Cavalli et al., 2017; Lague et al., 2013; Rączkowska & Cebulski, 2022) and could contribute to the future clarification of pros and cons of TLS application in debris flow/debris flood monitoring, and the assessment of the transferability of the of the methods to different regions.

2. Study area

The area of interest is located in the lower part of the river Damdere catchment, in the Eastern Rhodopes Mountains, Bulgaria (Figure 1). The total area of the catchment, delineated in GIS on the base of 30 m digital elevation model (DEM), is 39.3 km^2 and the relief is hilly or low mountainous.

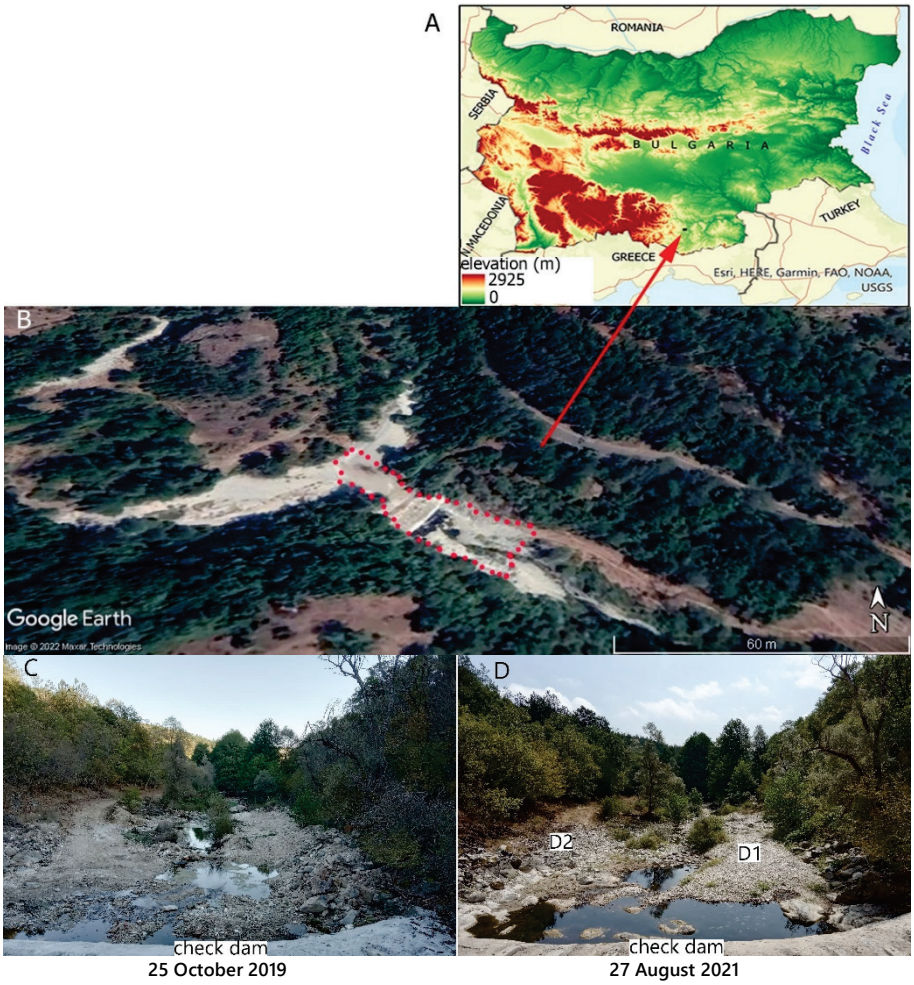

Figure 1. Location and view of the study area.

Note. Panel A: Location of the study area. Data used for the representation of terrain altitude are retrieved from *Shuttle Radar Topography Mission (SRTM) 1 Arc-Second Global data* [Data set], by United States Geological Survey, Earth Resources Observation and Science Center, 2014 (https://doi.org/10.5066/F7PR7TFT). In the public domain. Panel B: View of the river Damdere valley bottom. Satellite image (Location: 41°32′39″ N, 25°20′29″ E; Imagery date: 23.08.2021) is generated using Version 7.3.4.8642 of Google Earth Pro (2022). Copyright 2022 by Maxar Technologies. Panel C and D: Photos of the river Damdere bed immediately after the check dam—sediments that had been accumulated near the check dam (seen on the photo of October 2019) were washed down the river bed and well-expressed embankment can be seen on the photo of August 2021 (at the right part of the river bed—D1), also more coarse clasts are deposited on the left side—D2.

The river Damdere is a left tributary of the river Varbitsa and is characterized by intermittent streamflow, with its maximum in winter and it almost dries up in the summer months, which is typical for most of the small rivers in this region. This river regime is strongly related to the annual distribution of the rainfall and less to the snowmelt. There is no rain gauge station in the studied catchment, which is a limiting factor of studying climate-driven geomorphological processes. Viewed in a wider territorial scope, for the region of the Eastern Rhodopes the maximum of precipitation is in December–January and the minimum is in August (Topliiski, 2006). Based on Modified Furnier Index (MFI), Nikolova, Matev, and Pophristov (2021) state that in the area of Kardzhali (located near the study catchment), moderate or high erosivity of precipitation has been observed for the most of the years in the last decade.

The study area is characterized by diverse petrographic composition, which is a reflection of the geological settings at the whole catchment of the river Damdere. In petrographic aspects, the catchment of the river Damdere can be divided into two parts. The upper and middle part of the catchment is built mainly by biotite gneisses, Startsevska lithotectonic unit (Sarov, Jordanov, Valkov, Georgiev, Kamburov, Raeva, Grozdev, Balkanska, Moskovska, Dobrev, & Kalinova, 2007), while in the lower part of the catchment metagranites of Borovitsa lithotectonic unit and limestones of Kardzhali volcanic sedimentary group are predominant (Sarov, Jordanov, Valkov, Georgiev, Kamburov, Raeva, Grozdev, Balkanska, Moskovska, & Dobrev, 2007). Particularly at the studied downstream debris flood area the variety of the rocks is presented by metagranites, conglomerates and sandstones, but also biotite gneisses, quartzites, marbles, and organogenic limestones and tuffs can be found, which are transported from the upper part of the catchment area. The highly weathered rocks feed the sediment load of the water flow, which is favored by rare vegetation on some parts of the mountain slopes and high slope gradients. This, together with intensive rainfall, is a prerequisite for the frequent occurrence of debris floods. The river bed is covered by well-rounded gravel, pebbles, and boulders. The roundness, shape, and orientation of the clasts confirm the type of the hydrogeomorphological event to be a debris flood. Most of the clasts have disc and cylindrical shape and the long axes of the clasts are perpendicular or obliquely oriented to the direction of flow. The sediments sampling carried out in September 2020 and August 2021 show that pebble and sand fractions are predominant and take around 80–90%.

Several check dams were built in the lower and upper parts of the river Damdere valley to reduce the stream power and the sediment transport, and to minimize the risk of flooding. As a result of yearly occurrence of high water with high sediment load, the check dam in the lower part of the valley (the study area) is filled, which is a prerequisite for increasing the flood hazard and requires the analysis of the effectiveness of the protective facilities.

3. Data and methods

The area of interest is subject to monitoring since 2019. The field geomorphological observations and analyses are combined with TLS of the lower part of the river Damdere bed. In order to analyze the topographic change, two subsequent scanning of the debris flood area were carried out—in October 2019 and in August 2021.

3.1. Data acquisition and processing

The data acquisition was performed via medium-range laser scanner Stonex X300 in standard resolution mode (horizontal resolution—360° is 8,000 points; vertical resolution—90° is 2,000

points; total points per scan is 16,000,000). The terrain of the river Damdere basin required three laser scanning stations per campaign. Calibrated high-quality photos were obtained via a pair of internal cameras, which were then used to acquire RGB data for each point in the resulting point clouds. High-accuracy GNSS network RTK observations were performed on six vinyl targets placed homogeneously inside the scanning area for further georeferencing purposes.

The initial data processing was performed via the JRC 3D Reconstructor software (Gexcel Srl., 2016), Stonex version 3, education license, where the data from both campaigns were registered (using the cloud-to-cloud technique), combined and georeferenced in the WGS84 UTM 35 North projected coordinate system. The ground points were obtained by Cloth Simulation Filter with a cloth resolution 0.5 (Zhang et al., 2016) of point clouds in CloudCompare software (Version 2.12 beta; EDF R&D, 2022) and manual cleaning of vegetation was also done. The artificial concrete structures (check dam) were also removed manually from the point clouds. After this processing, two clean pairs of ground point clouds (obtained in 2019 and in 2021) were extracted: the first for the part before the check dam, and the second one—for that after the dam. These point clouds, saved in LAS format, were further processed in ArcGIS Pro 2.9.2 (ESRI, 2021) and high-resolution digital terrain models (DTMs) were created to be used for the analyses of the topographic change.

3.2. Topographic change detection and analysis

The topographic change in the studied areas was analyzed and evaluated in the following aspects:

- Multiscale Model to Model Cloud Comparison (M3C2; Lague et al., 2013); and
- DTMs analyses and calculation the volumes of erosion and deposition.

The M3C2 algorithm allows direct comparison of 3D TLS data without requiring gridding or meshing of the point cloud (Lague et al., 2013). The distance between the two successive point clouds is calculated along a normal vector for core points in a given scale. For the aim of our study, we used the cloud of the first scanning campaign (October 2019) as a reference cloud and accepted the all cloud as core points. The second cloud (of August 2021) is a comparable cloud. Taking into account the terrain morphometry, the normals calculation mode was set to vertical and only purely vertical normals were used.

DTMs with a cell size of 0.1 m were built in ArcGIS Pro (ESRI, 2021) by binning interpolation of point data (LAS files) from both TLS campaigns. The analysis was done separately for the part of the study area above the check dam (330 m^2) and for the lower part right after the check dam (623 m^2). The widely used method of DEM of difference (DoD) of the two consecutive models is used to evaluate short-term topographic change. This method presents the change of the topographic surface that is a result of the interpolation of point data. In this relation, the uncertainty of the results strongly depends on the quality of the initial data and the point density.

In addition to DoD, profile curvature rasters were also considered. They were generated in ArcGIS Pro (ESRI, 2021) environment on the base of DTMs. Profile curvature was calculated in the direction of maximal slope gradient and presented the distribution of concave and convex areas, which can be considered as indicators for erosion and deposition. The volumes of erosion and deposition were calculated on the base of the DTMs, which were created of the data acquired in both TLS campaigns.

4. Results and discussion

4.1. Topographic change evaluation by M3C2

The M3C2 algorithm was applied for both parts of the studied area (before and after the check dam) and as a result, the vertical distance between both clouds was calculated. In cases where there was no corresponding point to the compared cloud, no calculations were made (Figure 2A and 2B).

The reliability of the results strongly depends on the point density, vegetation, and the distance to the scanner. In this relation, the advantage of the used M3C2 algorithm was the calculation of the distance uncertainty. The obtained point density varied between 1 to 56,727 per m^2 for the part of the river bed before the check dam, and between 1 to 35705 per m^2 for part after the check dam.

The analysis of the upper part of the river bed shows that the distance values between 0.20 m and 0.17 m are predominant (nearly 92% of the calculations) and 23% of them are in the interval from –0.09 to 0.04 m. The highest values in the uppermost part of the considered area are most probably related to the influence of vegetation and some data imperfections, rather than real values (Figure 2A).

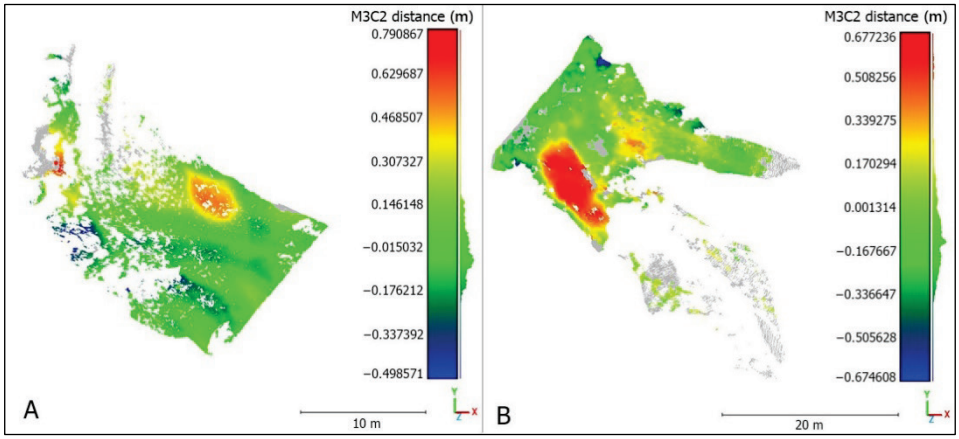

Figure 2. M3C2 distance (m): reference cloud—acquired October 2019; compared cloud—acquired April 2021 (print screen of CloudCompare, Version 2.12 beta).

Note. Panel A: The river Damdere bed before the check dam. Panel B: the river Damdere bed after the check dam. Gray color indicates no calculations due to non-interception between the clouds.

The calculated distance uncertainty is shown in Figure 3A. The lowest values present the highest reliability of the calculated distances. Uncertainty less than 5 mm is observed for 97% of the calculation and nearly 2.5% are with the uncertainty between 5 and 10 mm. M3C2 algorithm shows significant change for the most of the studied area before the check dam for the period October 2019–August 2021 (Figure 3B).

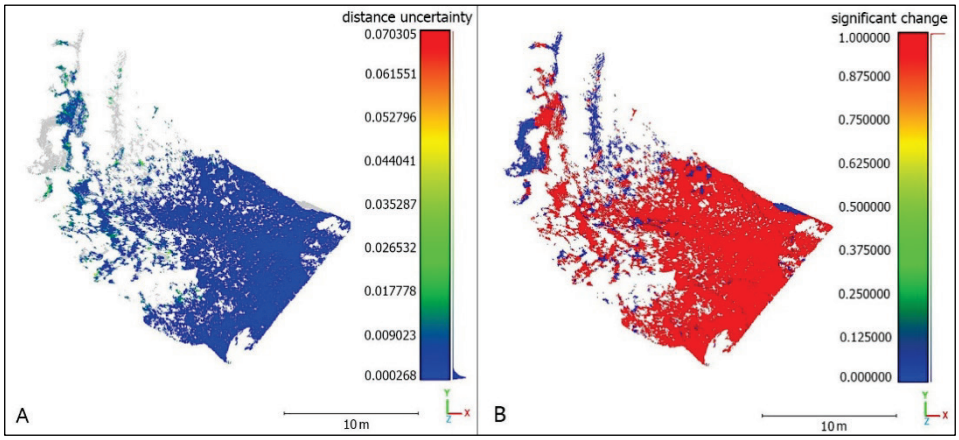

Figure 3. Statistical parameters of M3C2 for the area before the check dam (print screen of CloudCompare, Version 2.12 beta).

Note. Panel A: Distance uncertainty—the lower the values, the greater the accuracy of the calculations. Panel B: Significant change—red color = significant; blue color = non-significant.

The results of the comparison of both consecutive clouds after the check dam show a distance in the interval from –0.67 to 0.67 m (Figure 2B). The highest values have been observed at the right part of the river bed where gravels and pebbles are deposited. Another deposition area was also formed on the left side in the direction of the river bank and on the earth path, where the maximal deposition was 40 cm. High negative values (from –0.50 to –0.20 m) of the M3C2 distance were calculated near the check dam and partly on the left slope. Distances between –0.50 and –0.67 take 0.9% of the calculations and some of them are probably due to the effect of vegetation and applied filtering. Generally, the calculations are closely related to the hydrological conditions at the river bed. There was no stream flow during both TLS campaigns, but the size and the depth of the separate water areas were different (Figure 1C and 1D). The distance uncertainty is relatively high in the side parts most distant from the slope and in the parts of the valley bed, away from the scanner, where due to the vegetation, the surface visibility is the lowest. Despite this, regarding the whole area, the results show low distance uncertainty, which confirms the applicability of the M3C2 algorithm. In 49% of the calculations the value of uncertainty is less than 5 mm, and in 37% the uncertainty is less than 2 mm (Figure 4A). The surface change is significant at 85% of the M3C2 calculations (Figure 4B).

The analysis of the results of the application of M3C2 algorithm shows that the counts of the positive distances between both of the successive point clouds of the part above the check dam are greater than those after the check dam, but their values are lower and the differences between erosion and deposition in the upper part of the studied area (before the check dam) are less expressed. This indicates higher deposition rate after the check dam which have to direct the attention to the retaining capacity of the dam.

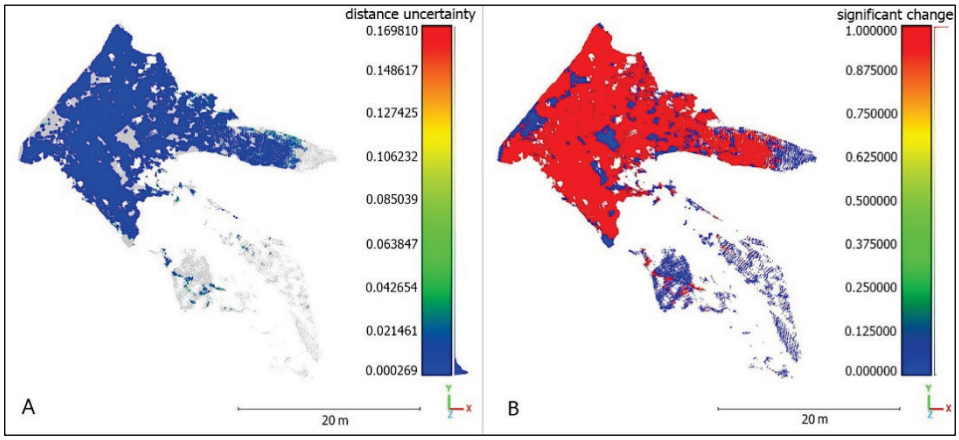

Figure 4. Statistical parameters of M3C2 for the area after the check dam (print screen of CloudCompare, Version 2.12 beta).

Note. Panel A: Distance uncertainty—the lower the values, the greater the accuracy of the calculations. Panel B: Significant change—red color = significant; blue color = non-significant.

4.2. Topographic change detection by DTMs analyses

DoDs for both parts of the valley bottom (before and after the check dam) show similar results (Figure 5A and 5B). Despite the relatively high rate of vertical differences between the 2019 DTM and 2021 DTM at the most of the terrain, the differences are between –0.1 and 0.1 m. Areas with washed sediment layer up to 10 cm thick take 25% of the studied area before the check dam and 22% of the area after the dam. The areas with a deposition up to 10 cm are 23% and 24%, respectively. The highest values of DoD (larger than 50 cm) are observed on very small parts of the models, which are particularly negligible for the areas of sediment washing (0.04% before the check dam and 0.4% after it). Limited areas show deposition higher than 50 cm (1.9% of the studied area before the check dam and 3.6% after it). The comparison of the topographic change of both parts of the valley bottom shows different patterns above and below the check dam. Generally, the distribution of the areas of erosion and deposition before the check dam shows 46% for erosion and 54% for deposition, while after the dam these areas take 41% and 59%, respectively. These values of the DoD indicate high sediment transport from the upper part of the river Damdere catchment and deposition at the lower valley where the velocity and the transport power of the stream flow are lower. This can also be seen in the volumes of erosion and deposition that have been calculated on the base of the DTMs. For the period October 2019–August 2021 the volume of the accumulated material is 29 m^3 before the check dam and 64.5 m^3 after it, while erosion is 17 m^3 and 32 m^3, respectively. Although the area for which the volume was calculated after the check dam is nearly 2 times larger than that above the concrete structure, the data related to the same area (per unit area) show a higher degree of accumulation after the check dam at almost the same slopes gradient of the river bed before and after the dam. This shows that the retention capacity of the dam has decreased which increases the flood hazard.

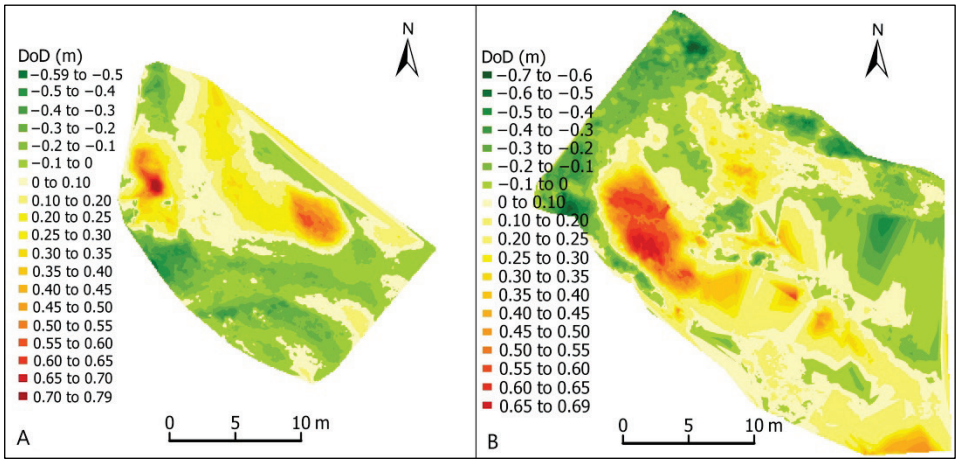

Figure 5. DEM of difference.

Note. Panel A: Before the check dam. Panel B: After the check dam.

Compared to the results of the M3C2 algorithm with vertical normal calculation, DoD shows nearly the same values of the topographic change. Despite the indisputable advantages of the M3C2 (Lague et al., 2013), DoD gives reliable results when it is applied to flat or near to flat areas in a small size. The model-to-model comparison reduces the impact of point cloud roughness on the accuracy of point cloud distance calculation (Li et al., 2021). Also, an advantage of DoD is easy calculation of volumes, but on the other side, in case of no data in some parts of the studied area due to vegetation or absence of visibility, the results depend on interpolation method and the resolution of the model. Although the mentioned imperfections of DoD, the method is widely used for the detection and evaluation of the geomorphic change (Cavalli et al. 2017; Heckmann & Vericat, 2018; James et al., 2012; Llena et al., 2020).

To determine the character of the geomorphic process (erosion or deposition), profile curvature rasters, which are second derivatives of DEM, are created and analyzed. The results show the decrease of the concave surfaces and the increase of the ones on the convex parts (Table 1). Despite the small differences in the areas, these results, interpreted in relation to the calculated volumes of erosion and deposition show that in both parts of the valley bottom deposition is greater than erosion.

Table 1. Changes of profile curvature in the lower valley of the river Damdere (% of the studied area)

Data acquisition	Before the check dam		After the check dam	
	Convex (%)	Concave (%)	Convex (%)	Concave (%)
October 2019	46	54	47	53
August 2021	49	51	49	51

The calculated topographic change for the period 27 October 2019–26 August 2021 is closely related to the cases of intensive rainfall in the river Damdere catchment and their distribution. According to the definitions of the European Climate Assessment & Dataset project (ECA&D, n.d.), days with precipitation over 20 mm are considered as very heavy precipitation days. Considering the daily precipitation data retrieved from National Institute of

Meteorology and Hydrology, Bulgaria (n.d.), the closely located rain gauge stations in Kardzhali (20 km) and Dzhebel (nearly 10 km) show that during the observed period, the total number of precipitation days is between 180 (Kardzhali) and 194 (Dzhebel). Daily precipitation amount above 20 mm was observed in 13% of precipitation days in Dzhebel and in 12% of the cases in Kardzhali, while precipitation fraction due to very heavy precipitation days is about 44% of the total amount of precipitation for the investigated period. These values indicate irregular distribution of the precipitation and cases of high precipitation for a short period which is a prerequisite for the occurrence of debris flows and debris floods. Similar results are obtained for the region Kresna Gorge (Western Bulgaria) by Krenchev et al. (2021), which gives reason to assume that daily precipitation above 20 mm could be considered as a threshold value for active hydrogeomorphological processes (debris flows/debris floods). Having regard to the peculiarities and differences in land cover and hydrological conditions, further investigations are needed to specify the impact of weather conditions on short-term geomorphic change.

5. Conclusion

The field observations and measurements, as well as the analyses of the point clouds obtained during the field TLS campaigns, show active hydrogeomorphic process in the low valley of the river Damdere catchment. Debris floods are triggered by intensive rainfall and high sediment loads are accumulated in the flat river bed before and after the check dam. The short-term topographic change is evaluated by successive TLS of the area near the check dam. The 3D point clouds are analyzed having regard to the geomorphological observations that were carried out simultaneously with the scanning. Despite the retaining role of the check dam, the application of M3C2 algorithm and the analysis of the results give grounds to conclude that the deposition is larger at the lower part of the river bed after the check dam. Similar results are obtained by differencing the successive DTMs. DoD approach shows that the topographic changes in the larger part of the studied area are between –0.1 and 0.1 m for the period October 2019–August 2021. High values of accumulation are observed in the lateral parts of the river bed, which is an indicator of turbulent character of the flow. The areas before the check dam where the washing of sediments is observed are 46% while the deposition takes 54%. After the dam, these areas take 41% and 59% respectively.

Despite the different approaches in calculation the topographic change and the impact of interpolation method and model resolution on topographic change detection, M3C2 algorithm and DoD show very similar results when they are applied to the relatively flat and small areas of the river valley bottom.

The presented study is the first one for the considered area, performed on the basis of two consecutive TLS campaigns over nearly two years. In relation to the point clouds analysis and derivative models, future research will focus on more detailed evaluation of DTMs uncertainty and the impact of model resolution on topographic change detection.

Acknowledgements

This work has been carried out in the framework of the National Science Program "Environmental Protection and Reduction of Risks of Adverse Events and Natural Disasters", approved by the Resolution of the Council of Ministers No. 577/17.08.2018 and supported by the Ministry of Education and Science (MES) of Bulgaria (Agreement No. Д01-279/03.12.2021)

References

Aigner, P., Kuschel, E., Zangerl, C., Hübl, J., Hrachowitz, M., Sklar, L., & Kaitna, R. (2021, April 19–30). *Multi-sensor approach towards understanding debris-flow activity in the Lattenbach catchment, Austria*. EGU General Assembly 2021, EGU21-15399, https://doi.org/10.5194/egusphere-egu21-15399

Baltakova, A., Nikolova, V., Kenderova, R., & Hristova, N. (2018). Analysis of debris flows by application of GIS and remote sensing: case study of western foothills of Pirin Mountain (Bulgaria). In S. S. Chernomorets & G. V. Gavardashvili (Eds.), *Debris Flows: Disasters, Risk, Forecast, Protection. Proceedings of the 5th International Conference* (pp. 22–32). Publishing House "Universal". http://www.debrisflow.ru/wp-content/uploads/2018/10/Baltakova_DF18.pdf

Blasone, G., Cavalli, M., Marchi, L., & Cazorzi, F. (2014). Monitoring sediment source areas in a debris-flow catchment using terrestrial laser scanning. *Catena*, *123*, 23–36. http://dx.doi.org/10.1016/j.catena.2014.07.001

Bovis, M. J., & Jakob, M. (1999). The role of debris supply conditions in predicting debris flow activity. *Earth Surface Processes and Landforms*, *24*(11), 1039–1054. https://doi.org/10.1002/(SICI)1096-9837(199910)24:11<1039::AID-ESP29>3.0.CO;2-U

Bruchev, Il., Frangov, G., & Yanev, Y. (2001). Katastrofalni yavleniya v Iztochnite Rodopi [Catastrophic phenomena in the Eastern Rhodopes]. *Mining and geology*, *6*, 33–36.

Cavalli, M., Goldin, B., Comiti, F., Brardinoni, F., & Marchi, L. (2017). Assessment of erosion and deposition in steep mountain basins by differencing sequential digital terrain models. *Geomorphology*, *291*, 4–16. https://doi.org/10.1016/j.geomorph.2016.04.009

Costa, J. E. (1984). Physical geomorphology of debris flows. In J. E. Costa & P. J. Fleisher (Eds.), *Developments and applications of geomorphology* (pp. 268–317). Springer. https://doi.org/10.1007/978-3-642-69759-3_9

Costa, J. E. (1988). Rheologic, geomorphic, and sedimentologic differentiation of water floods, hyperconcentrated flows, and debris flows. In V. R. Baker, R. C. Kochel, & P. C. Patton (Eds.), *Flood Geomorphology* (pp. 113–122). Wiley.

Dhote, P. R., Thakur, P. K., Chouksey, A., Srivastav, S. K., Raghvendra, S., Rautela, P., Ranjan, R., Allen, S., Stoffel, M., Bisht, S., Negi, B. S., Aggarwal, S. P., & Chauhan, P. (2022). Synergistic analysis of satellite, unmanned aerial vehicle, terrestrial laser scanner data and process-based modelling for understanding the dynamics and morphological changes around the snout of Gangotri Glacier, India. *Geomorphology*, *396*, Article 108005. https://doi.org/10.1016/j.geomorph.2021.108005

Dobrev, N., & Georgieva, M. (2010). Kalno-kamenniteporoi v severnata chast na Kresnenskoto defile: harakteristika na zonata na podhranvane i svoistva na izgrazhdashtite ya materiali [The debris flow in the northern part of Kresna Gorge: characterization of the source zone and material properties]. *Review of the Bulgarian Geological Society*, *71*(1–3), 113–121. http://dx.doi.org/10.13140/RG.2.1.1314.1601

Dobrev, N., Ivanov, P., Varbanov, R., Frangov, G., Berov, B., Bruchev, I., Krastanov, M., & Nankin, R. (2013). Landslide Problems in Bulgaria: Factors, Distribution and Countermeasures. In C. Margottini, P. Canuti, K. Sassa (Eds.), *Landslide Science and Practice: Vol. 7. Social and Economic Impact and Policies* (pp. 187–193). Springer. https://doi.org/10.1007/978-3-642-31313-4_24

Dotseva, Z., Vangelov, D., & Gerdjikov, I. (2021). Proyava na kalno-kamenni pototsi I debritni priizhdaniq vav vodosbora na rka Ribnishka (yuzhnite sklonove na Ograzhden) [Debris flows and debris floods occurrence in the Ribnishka River watershed (southern slopes of Ograzhden Mountain)]. *Review of the Bulgarian Geological Society*, *82*(3), 165–167. https://doi.org/10.52215/rev.bgs.2021.82.3.165

European Climate Assessment & Dataset. (n.d.). *Indices dictionary*. ECA&D. https://www.ecad.eu/indices extremes/indicesdictionary.php

EDF R&D. (2022). *CloudCompare* (Version 2.12 beta) [GPL software]. https://www.cloudcompare.org/

ESRI. (2021). ArcGIS Pro 2.9 [Computer software]. Environmental Systems Research Institute. https://www.esri.com/en-us/home

Gexcel Srl. (2016). *JRC 3D Reconstructor 3* (Version 3.2.1.584) [Computer software]. https://www.geo3d.hr/software/gexcel/jrc-3d-reconstructorr

Google Earth Pro (Version 7.3.4.8642) [Computer software]. (2022). https://www.google.com/intl/en/earth/versions/

Heckmann, T., & Vericat, D. (2018). Computing spatially distributed sediment delivery ratios: inferring functional sediment connectivity from repeat high-resolution digital elevation models. *Earth Surface Processes and Landforms*, *43*(7), 1547–1554. https://doi.org/10.1002/esp.4334

Ilinca, V. (2021). Using morphometrics to distinguish between debris flow, debris flood and flood (Southern Carpathians, Romania). *Catena*, *197*, Article 104982. https://doi.org/10.1016/j.catena.2020.104982

Jackson, L. E., Kostaschuk, R. A., & MacDonald, G. M. (1987). Identification of debris flow hazard on alluvial fans in the Canadian Rocky Mountains. In J. E. Costa & G. F. Wieczorek (Eds.), *Debris Flows/Avalanches: Process, Recognition, and Mitigation* (pp. 115–124). Geological Society of America. https://doi.org/10.1130/REG7-p115

James, L. A., Hodgson, M. E., Ghoshal, S., & Latiolais, M. M. (2012). Geomorphic change detection using historic maps and DEM differencing: The temporal dimension of geospatial analysis. *Geomorphology*, *137*(1), 181–198. https://doi.org/10.1016/j.geomorph.2010.10.039

Kamburov, A., & Nikolova, V. (2020). 3D modelling in GIS environment for the purpose of debris flow analysis – a case study of the Eastern Rhodopes (Bulgaria). In T. Bandrova, M. Konečný, & S. Marinova (Eds.), *8th International Conference on Cartography and GIS* (Vol. 1, pp. 278–286). Bulgarian Cartographic Association. https://iccgis2020.cartography-gis.com/8ICCGIS-Vol1/8ICCGIS_Proceedings_Vol1_2020-Optimized.pdf

Keilig, K., Dietrich, A., & Krautblatter, M. (2018). How to effectively monitor geomorphic changes in debris-flow channels. In S. S. Chernomorets & G. V. Gavardashvili (Eds.), *Debris Flows: Disasters, Risk, Forecast, Protection. Proceedings of the 5th International Conference* (pp. 123–129). Publishing House "Universal". http://www.debrisflow.ru/wp-content/uploads/2018/10/Keilig_DF18.pdf

Kenderova, R., Baltakova, A., & Ratchev, G. (2013). Debris Flows in the Middle Struma Valley, Southwest Bulgaria. In D. Lóczy (Ed.), *Geomorphological Impacts of Extreme Weather: Case Studies from Central and Eastern Europe* (pp. 281–297). https://doi.org/10.1007/978-94-007-6301-2_18

Krenchev, D., Kenderova, R., Matev, S., Nikolova, N., Rachev, G., & Gera, M. (2021). Debris Flows in Kresna Gorge (Bulgaria)—Geomorphological Characteristics and Weather Conditions. *Journal of the Geographical Institute "Jovan Cvijić" SASA, 71*(1), 15–27. https://doi.org/10.2298/IJGI2101015K

Lague, D., Brodu, N., & Leroux, J. (2013). Accurate 3D comparison of complex topography with terrestrial laser scanner: Application to the Rangitikei canyon (N-Z). *ISPRS Journal of Photogrammetry and Remote Sensing*, *82*, 10–26. https://doi.org/10.1016/j.isprsjprs.2013.04.009

Li, Y., Liu, P., Li, H., & Huang, F. (2021). A Comparison Method for 3D Laser Point Clouds in Displacement Change Detection for Arch Dams. *ISPRS International Journal of Geo-Information*, *10*(3), Article 184. https://doi.org/10.3390/ijgi10030184

Llena, M., Vericat, D., Smith, M. W., & Wheaton, J. M. (2020). Geomorphic process signatures reshaping sub-humid Mediterranean badlands: 1. Methodological development based on high-resolution topography. *Earth Surface Processes and Landforms*, *45*(5), 1335–1346. https://doi.org/10.1002/esp.4821

Loye, A., Jaboyedoff, M., Theule, J. I., & Liébault, F. (2016). Headwater sediment dynamics in a debris flow catchment constrained by high-resolution topographic surveys. *Earth Surface Dynamics*, *4*(2), 489–513. https://doi.org/10.5194/esurf-4-489-2016

National Institute of Meteorology and Hydrology, Bulgaria. (n.d.). Daily precipitation data retrieved daly for the period 25.10.2019 – 27.08.2021. https://hydro.bg/bg/t1.php?ime=&gr=data/&gn=dajd

Nikolova, V., Kamburov, A., & Rizova, R. (2020). Modelling and assessment of debris flow erosion and deposition using geoinformation technologies. *Journal of Mining and Geological Sciences*, *63*, 232–237. https://mgu.bg/wp-content//uploads/resources/Journal-of-MG-Sciences-63-2020.pdf

Nikolova, V., Kamburov, A., & Rizova, R. (2021). Morphometric analysis of debris flows basins in the Eastern Rhodopes (Bulgaria) using geospatial technologies. *Natural Hazards*, *105*, 159–175, https://doi.org/10.1007/s11069-020-04301-4

Nikolova, N., Matev, S., & Pophristov, V. (2021). Rainfall erosivity and extreme precipitation months – a comparison between the regions of Lovech and Kardzhali (Bulgaria). In O. Trofymchuk & B. Rivza (Eds.), *21st International Multidisciplinary Scientific GeoConference SGEM 2021* (Vol. 21, Book 3.1, pp. 389–396). https://doi.org/10.5593/sgem2021/3.1/s13.64

Petrović, A., Kostadinov, S., & Dragićević, S. (2014). The Inventory and Characterization of Torrential Flood Phenomenon in Serbia. *Polish Journal of Environmental Studies*, *23*(3), 823–830. http://www.pjoes.com/pdf-89253-23111?filename=The%20Inventory%20and.pdf

Petrović, A. M., Novković, I., & Kostadinov, S. (2021). Hydrological analysis of the September 2014 torrential floods of the Danube tributaries in the Eastern Serbia. *Natural Hazards*, *108*, 1373–1387. https://doi.org/10.1007/s11069-021-04737-2

Picco, L., Mao, L., Cavalli, M., Buzzi, E., Rainato, R., & Lenzi, M. A. (2013). Evaluating short-term morphological changes in a gravel-bed braided river using terrestrial laser scanner. *Geomorphology*, *201*, 323–334. https://doi.org/10.1016/j.geomorph.2013.07.007

Pierson, T. C. (2005). *Distinguishing between debris flows and floods from field evidence in small watersheds* [Fact Sheet 2004-3142]. United States Geological Survey. https://doi.org/10.3133/fs20043142

Pierson, T., & Costa, J. (1987). A rheologic classification of subaerial sediment-water flows. In J. E. Costa & G. F. Wieczorek (Eds.), *Debris Flows/Avalanches: Process, Recognition, and Mitigation* (Vol. 7, pp. 1–12). Geological Society of America.

Rączkowska, Z., & Cebulski, J. (2022). Quantitative assessment of the complexity of talus slope morphodynamics using multi-temporal data from terrestrial laser scanning (Tatra Mts., Poland). *Catena*, *209*(Part 1), Article 105792. https://doi.org/10.1016/j.catena.2021.105792

Rainato, R., Picco, L., Cavalli, M., Mao, L., Delai, F., Ravazzolo, D., & Lenzi, M. A. (2013). Evaluation of short-term geomorphic changes along the Tagliamento river using LiDAR and terrestrial laser scanner surveys. *Journal of Agricultural Engineering*, *44*(s2), 80–84. https://doi.org/10.4081/jae.2013.256

Rizova, R., & Nikolova, V. (2021). Geomorphological and sedimentological characteristics of debris lows in the river Buyukdere watershed (Eastern Rhodopes, Bulgaria). In O. Trofymchuk & B. Rivza (Eds.), *21st International Multidisciplinary Scientific GeoConference SGEM 2021* (pp. 43–50). STEF92 Technology. https://doi.org/10.5593/sgem2021/1.1/s01.007

Sarov, S., Jordanov, B., Valkov, V., Georgiev, S., Kamburov, D., Raeva, E., Grozdev, V., Balkanska, E., Moskovska, L., Dobrev, G., & Kalinova, I. (2007). *Geological Map of Republic of Bulgaria, Scale 1:50000* (Map sheet Ardino). Ministry of Environment and Water, Bulgarian Geological Survey.

Sarov, S., Jordanov, B., Valkov, V., Georgiev, S., Kamburov, D., Raeva, E., Grozdev, V., Balkanska, E., Moskovska, L., & Dobrev, G. (2007). *Geological Map of Republic of Bulgaria, Scale 1:50000* (Map sheet Kardzgaly). Ministry of Environment and Water, Bulgarian Geological Survey.

Schürch, P., Densmore, A. L., Rosser, N. J., Lim, M., & McArdell, B. (2011). Detection of surface change in complex topography using terrestrial laser scanning: application to the Illgraben debris-flow channel. *Earth Surface Processes and Landforms,* 36(14), 1847–1859. https://doi.org/10.1002/esp.2206

Slaymaker, O. (1988). The distinctive attributes of debris torrents. *Hydrological Sciences Journal, 33*(6), 567–573. https://doi.org/10.1080/02626668809491290

Topliiski, D. (2006). *Klimat na Balgaria* [Climate of Bulgaria]. Amstels Foundation

United States Geological Survey, Earth Resources Observation and Science Center. (2014). *Shuttle Radar Topography Mission (SRTM) 1 Arc-Second Global data* [Data set]. https://doi.org/10.5066/F7PR7TFT

Wilford, D. J., Sakals, M. E., Innes, J. L., Sidle, R. C., & Bergerud, W. A. (2004). Recognition of debris flow, debris flood and flood hazard through watershed morphometrics. *Landslides, 1*, 61–66. https://doi.org/10.1007/s10346-003-0002-0

Zhang, W., Qi, J., Wan, P., Wang, H., Xie, D., Wang, X., & Yan, G. (2016). An Easy-to-Use Airborne LiDAR Data Filtering Method Based on Cloth Simulation. *Remote Sensing*, *8*(6), Article 501. https://doi.org/10.3390/rs8060501

Zhou, W., Tang, C., Van Asch, T. W. J., & Chang, M. (2015). A rapid method to identify the potential of debris flow development induced by rainfall in the catchments of the Wenchuan earthquake area. *Landslides, 13*, 1243–1259. https ://doi.org/10.1007/s1034 6-015-0631-0